high grade gliomas. *J Neurooncol* 2002; 59: 81–90.

9. Nakada K, Katoh C, Kanegae K, Tsukamoto E, Itoh K, Furudate M, et al. The role of ^{201}Tl scintigraphy in evaluating proliferative activity in thyroid neoplasms. *Ann Nucl Med* 1996; 10: 41–48.

10. Suga K, Kume N, Orihashi N, Nishigauchi K, Uchisako H, Matsumoto T, et al. Difference in ^{201}Tl accumulation on single photon emission computed tomography in benign and malignant thoracic lesions. *Nucl Med Commun* 1993; 14: 1071–1078.

11. Kaplan WD, Takvorian T, Morris JH, Rumbaugh CL, Connolly BT, Atkins HL. Thallium-201 brain tumor imaging: A comparative study with pathologic correlation. *J Nucl Med* 1987; 28: 47–52.

12. Vertosick FT Jr, Selker RG, Grossman SJ, Joyce JM. Correlation of thallium-201 single photon emission computed tomography and survival after treatment failure in patients with glioblastoma multiforme. *Neurosurgery* 1994; 34: 396–401.

13. Lorberboym M, Mandell LR, Mosesson RE, Germano I, Lou W, DaCosta M, et al. The role of thallium-201 uptake and retention in intracranial tumor after radiotherapy. *J Nucl Med* 1997; 38: 223–226.

14. Rodrigues M, Fonseca AT, Salgado D, Vieira MR. ^{99m}Tc-HMPAO brain SPECT in the evaluation of prognosis after surgical resection of astrocytoma. Comparison with other noninvasive imaging techniques (CT, MRI and ^{201}Tl SPECT). *Nucl Med Commun* 1993; 14: 1050–1060.

15. Black KL, Emerick T, Hoh C, Hawkins RA, Mazziotta J, Becker DP. Thallium-201 SPECT and positron emission tomography equal predictors of glioma grade and recurrence. *Neurol Res* 1994; 16: 93–96.

16. Bénard F, Romsa J, Hustinx R. Imaging gliomas with positron emission tomography and single-photon emission computed tomography. *Semin Nucl Med* 2003; 33: 148–162.

17. Oriuchi N, Tamura M, Shibazaki T, Ohye C, Watanabe N, Tateno M, et al. Clinical evaluation of thallium-201 SPECT in supratentorial gliomas: Relationship to histologic grade, prognosis and proliferative activities. *J Nucl Med* 1993; 34: 2085–2089.

18. Higa T, Maetani S, Kobashi Y, Nabeshima S. Tl-201 SPECT compared with histopathologic grade in the prognostic assessment of cerebral gliomas. *Clin Nucl Med* 2001; 26: 119–124.

19. Kosuda S, Fujii H, Aoki S, Suzuki K, Tanaka Y, Nakamura O, et al. Prediction of survival in patients with suspected recurrent cerebral tumors by quantitative thallium-201 single photon emission computed tomography. *Int J Radiat Oncol Biol Phys* 1994; 30: 1201–1206.

20. Black KL, Hawkins RA, Kim KT, Becker DP, Lerner C, Marciano D. Use of thallium-201 SPECT to quantitate malignancy grade of gliomas. *J Neurosurg* 1989; 71: 342–346.

21. Jinnouchi S, Hoshi H, Ohnishi T, Futami S; Nagamachi S, Watanabe K, et al. Thallium-201 SPECT for predicting histological type of meningiomas. *J Nucl Med* 1993; 34: 2091–2094.

22. Sun D, Liu Q, Liu W, Hu W. Clinical application of ^{201}Tl SPECT imaging of brain tumor. *J Nucl Med* 2000; 41: 5–10.

23. Baumert BG, Lutterbach J, Bernays R, Davis JB, Heppner FL. Fractionated stereotactic radiotherapy boost after postoperative radiotherapy in patients with high-grade gliomas. *Radiother Oncol* 2003; 67: 183–190.

24. Thilmann C, Zabel A, Grosser KH, Hoess A, Wannenmacher M, Debus J. Intensity-modulated radiotherapy with an integrated boost to the macroscopic tumor volume in the treatment of high-grade gliomas. *Int J Cancer* 2001; 96: 341–349.

25. Kim S, Chung JK, Im SH, Jeong JM, Lee DS, Kim DG, et al. ^{11}C-methionine PET as a prognostic marker in patients with glioma: comparison with ^{18}F-FDG PET. *Eur J Nucl Med Mol Imaging* 2005; 32: 52–59.

ScienceDirect   日本語サポート

Home   Browse   Search   My Settings   Alerts   Help

Quick Search   Title, abstract, keywords   Author   e.g. j s smith

☑ search tips   Journal/book title   Volume   Issue   Page   Clear ☒   Go ☺

Heterogeneity of posterior limbic perfusion in very early Alzheimer's disease

This Document
- SummaryPlus
- ▶ **Full Text + Links**
  - ·Thumbnail Images
- PDF (266 K)

Actions
- Cited By
- Save as Citation Alert
- E-mail Article
- Export Citation
- ⟨ᴬ⟩ Add to my Quick Links

Michinobu Nagao[a], ☒, Yoshifumi Sugawara[a], Manabu Ikeda[b], Ryuji Fukuhara[b], Tomohisa Ishikawa[b], Kenya Murase[c], Takanori Kikuchi[a], Teruhito Mochizuki[a] and Hitoshi Miki[a]

[a]Department of Radiology, Ehime University Medical School, Japan
[b]Department of Neuropsychiatry, Ehime University Medical School, Japan
[c]Department of Medical Engineering, Division of Allied Health Sciences, Osaka University Medical School, Japan

Abstract

Purpose

This study was designed to quantify the heterogeneity of cerebral perfusion on SPECT images in elderly controls and Alzheimer's disease (AD) patients in mild stage using a three-dimensional fractal analysis (3D-FA).

Material and method

Seventy-five patients with possible and probable AD based on the NINCDS/ADRDA criteria, and thirty-one elderly controls underwent ^{99m}Tc-HMPAO SPECT scanning. Dementia severity was assessed using the clinical dementia rating (CDR). Patients with CDR scores of 0.5 ($n = 33$) were classified as "very early" and those with CDR 1 ($n = 42$) as "early". We delineated the SPECT images using 2 cutoffs (35% and 50% cutoffs of the maximal voxel radioactivity) and measured the number of voxels in the areas included by the contours obtained with each cutoff level. The fractal dimension (FD) was calculated by relating the logarithms of cutoff level and the number of voxels. Posterior limbic images were reconstructed at 30° positive to the coronal plane, and posterior limbic FD was calculated.

Result

Posterior limbic FD for early AD, very early AD, and control groups were 1.03 ± 0.16, 1.02 ± 0.17, and 0.87 ± 0.14 ($P = 0.001$ versus early AD group, $P = 0.001$ versus very early AD). Use of the posterior limbic FD and the ratio of posterior limbic FD to total FD

separated very early AD patients from controls with a sensitivity of 76% and a specificity of 81%.

Conclusion

3D-FA indicated significant differences in the heterogeneity of CBF distribution between patients with AD in mild stage and elderly controls. Posterior limbic FD may be useful for easily and objectively distinguishing patients with very early AD from aging people.

Keywords: Alzheimer's disease; Aging; SPECT; Cerebral perfusion; Fractal dimension

Article Outline

The most common neurodegenerative cause of dementia in the elderly is Alzheimer's disease (AD) (Kokmen et al., 1993). Memory impairment is usually the earliest manifestation, and differentiating the gradual decline in memory efficiency associated with healthy aging from mild AD is a diagnostic difficulty (Petersen et al., 1994). As effective treatments begin to emerge, detecting AD in the preclinical or very early clinical stage will become crucial. Thus, the development of neuroimaging markers offers one possible way forward.

PET and SPECT are useful imaging modalities for diagnosis and monitoring progression in AD. Cerebral blood flow (CBF) reductions in AD have a regionally dependent time course. In mild stages of the disease, CBF in the temporo-parietal region declines first, and regional CBF decrease spreads to frontal and other brain regions later (Foster et al., 1984, Haxby et al., 1985, Holman et al., 1992, Messa et al., 1994 and Nebu et al., 2001). However, the CBF in sensorimotor cortex, pons, and cerebellum are relatively preserved (Minoshima et al., 1997, Johnson et al., 1998 and Kogure et al., 2000). As regional CBF variability increases with progressing AD, we hypothesized that CBF distribution in very mild AD may also be more heterogeneous than that in healthy aging people.

Three-dimensional fractal analysis (3D-FA), based on an intensity threshold at different cutoffs for the involved area, was used to quantify the heterogeneous distribution on SPECT (Nagao et al., 2001, Yoshikawa et al., 2003a and Yoshikawa et al., 2003b). 3D-FA is a simple and objective image-analyzed method and is a helpful tool used to characterize CBF distribution patterns, which is not easy to diagnose through conventional visual analysis. In this study, we quantified the heterogeneous distribution on CBF SPECT images in very early AD, early AD, and healthy aging people using 3D-FA and examined the usefulness of the quantification for distinguishing these three groups.

1. Methods

1.1. Recruitment and characterization of subjects

Patients with cognitive impairment and the cognitively normal elderly were consecutively recruited from the Higher Brain Function Clinic at Ehime University Hospital between January 1998 and June 2003. All procedures used in this study were performed strictly according to the local Ethics Committee's Clinical Study Guidelines and were approved by the internal review board. Written informed consent was obtained from all participants or their caregivers after a complete description of the study.

Patients suspected of having cognitive impairment underwent detailed physical, neurological, and psychiatric examinations. Laboratory studies obtained from all patients included biochemistry, complete blood count, sedimentation rate, syphilis serology, sensitive thyroid-stimulating hormone, vitamin B12, folic acid, EEG, and brain MRI. Patients with MRI evidence of focal brain lesions and MR angiographic evidence of occlusive lesions in the cervical and intracranial arteries were excluded. MRI was performed with a 1.5T system (Gyroscan ACS-NT release 6, Philips, The Netherlands) incorporating a circularized head coil. The scanning parameters for T2-weighted turbo SE sequences were as follows: repetition time = 4.26 ms; effective echo time = 110 ms; echo train length = 10; matrix = 247 × 512; field of view = 220 mm; section thickness = 6 mm; intersection gap = 0.6 mm; NSA = 2; and imaging time = 2 min 54 s. Patients with only age-related hyperintensity lesions (less than 5 mm × 5 mm) in basal ganglia and white matter were included in this study (Drayer, 1988).

For diagnostic and research purposes, the patients were assessed with a comprehensive neuropsychological test battery, including mini-mental state examination (MMSE) (Folstein et al., 1975), Raven's coloured progressive matrices (RCPM) (Aftanas and Royce, 1969), the Alzheimer's disease assessment scale, cognitive subscale (ADAS-cog) (Mohs et al., 1983). Their principal caregivers were interviewed using the instrumental activities of daily living scale (IADL) and the physical self-maintenance scale (PSMS) (Lawton and Brody, 1969). Affective and behavioral disorders were evaluated using the neuropsychiatric inventory (NPI) (Cummings et al., 1994) for caregivers.

Following the completion of this evaluation, a consensus committee consisting of consultant neuropsychiatrists and consultant neurologists was convened to determine the clinical diagnosis. The clinical diagnosis of possible or probable AD was based on the National Institute of Neurological and Communicative Disorders/Stroke and Alzheimer's Disease and Related Disorders Association (NINCDS/ADRDA) criteria (McKhann et al., 1984). Dementia severity was assessed using the clinical dementia rating (CDR) (Morris, 1993). Patients with CDR 0.5 were classified as "very early" and those with CDR 1 as "early" (Table 1).

Table 1.

Subject characteristics

Characteristic	Control	Very early AD	Early AD
No.	31	33	42
Age (years)	73.3 ± 4.5	73.7 ± 5.8	74.1 ± 5.8
Education (years)	11.2 ± 2.6	10.9 ± 2.4	9.6 ± 2.4
Male/female	9/22	14/19	14/28
CDR	0	0.5	1
MMSE score	28.0 ± 1.8	23.2 ± 3.1	18.8 ± 3.6
RCPM		26.0 ± 3.5	20.7 ± 7.1
ADAS cognitive subscale		12.6 ± 6.9	18.8 ± 7.5

All patients have participated in a longitudinal project investigating aspects of cognition and behavior. Patients underwent clinical and neuropsychological reevaluations at approximately

12-month intervals. At first assessment the only major cognitive impairment in the patients with CDR 0.5 was memory disturbance with mild secondary disorientation (i.e. possible AD in NINCDS/ADRDA criteria). They had histories of progressive memory decline in the preceding 2–3 years as reported by their caregivers. With subsequent follow-up, their cognitive impairment progressed to the point where they all met NINCDS/ADRDA criteria for probable AD. Therefore, all of the AD cases (both very early and early) eventually diagnosed as probable AD. The mean follow-up time for these patients was 33.5 ± 17.9 months. This project included the patients with CDR 0.5, who had an unchanged cognitive impairment during follow up period. These patients did not meet NINCDS/ADRDA criteria for probable AD with subsequent follow-up. They were characterized as having stable mild cognitive impairment (MCI) or MCI not converted AD. These stable MCI patients were not included in AD and control groups.

Control subjects were derived from the same community population as the cognitively impaired subjects. These individuals underwent an evaluation similar to that described previously, including a general medical examination and part of the neuropsychological test battery mentioned above. Subjects qualified as normal controls if, in the opinion of their clinicians, they were functioning normally in the community and did not have any cognitive impairments. They could not have had any active neurologic or psychiatric illnesses and could not be taking any psychotropic medications (Table 1).

Age, education years, and sex ratios (males/females) were not statistically different among these three (two patient's and control) groups.

A CBF SPECT examination was performed within a month of the initial clinical assessment in all patients.

1.2. Data acquisition

Hexamethyl propyleneamine oxime (HMPAO) was labeled with ^{99m}Tc on site shortly before administration. The dose was approximately 740 MBq. The radiopharmaceutical was injected into an antecubital vein while the subjects lay supine with eyes closed in a secluded examination room. Data acquisition started at 10 min post-injection. A SPECT scanner (SPECT-2000H; Hitachi Medical Corp., Tokyo, Japan), incorporating a four-headed rotating gamma camera with an in-plane and axial resolution of 7.5 mm full width at half maximum (FWHM), equipped with low-energy high-resolution collimators for ^{99m}Tc in air, was used. Data were obtained from the 140keV photo peak (20% window) over 360° rotation using a 128 × 128 matrix. A step and shoot format was utilized with an acquisition time of 20 s/frame and a zoom factor of 1.33. Image reconstruction was performed by the filtered backprojection method using a Butterworth filter (order 10, cut-off frequency 0.12 cycles/pixel). Attenuation correction was performed using Chang's method by assuming the object shape to be an ellipse for each slice and the attenuation coefficient to be uniform (0.08 cm^{-1}). Slice thickness was 2 mm (one pixel).

1.3. Three-dimensional fractal analysis

Fractals were introduced by Mandelbrot (1967) to characterize structures and processes occurring in nature. The principal features of fractal objects are: (1) a large degree of heterogeneity, (2) scaling similarity over many scales of observation, and (3) the lack of a well-defined scale (Nelson, 1990). Fractal geometry is characterized where the relationship between a measure (M) and the scale (ε) is expressed as

$$M(\varepsilon)=k\varepsilon^{-D},\qquad(1)$$

where k is a scaling constant and D is called the fractal dimension (Nelson, 1990). As this equation implies, the quantity M to be measured is a function of the ruler scale and can be a non-constant. The fractal dimension is one parameter that is useful for this purpose in characterizing organizationally complex structures (Nelson, 1990). The fractal dimension is

a scale-independent measure of spatial heterogeneity.

In 3D-FA, the chosen cutoffs were used as the ruler scale r in Eq. (1), and the number of voxels with radioactivity higher than the corresponding cutoffs were expressed as $M(r)$. Clearly, $M(r)$ decreases as r increases; hence a linear regression on the $M(r)$ versus r graph, when plotted on a logarithm versus a logarithm scale, yielding a negative slope with the magnitude equal to the fractal dimension (Nagao and Murase, 2002 and Nagao et al., 2004).

In this study, we delineated the SPECT images using a 35% and a 50% cutoff of the maximal voxel radioactivity and measured the number of voxels included in the contours of the two different cut-offs. The fractal dimension (FD) was calculated by relating the logarithms of the cut-offs and the number of voxels based on the above equation and to define the heterogeneity of cerebral perfusion.

The important factor for 3D-FA is the range of cutoff levels used. In HMPAO SPECT studies, when a cut-off of less than 30% is used, artifactual regions outside the brain tend to be delineated, especially in younger patients. In this study, we targeted the reduction of cortical CBF because the first affected brain structure with progressing AD is the cerebral cortex. Thus, we selected the range of cut-off levels, which is expressed as the change of cortical CBF, and defined cut-off levels as 35% and 50% (Nagao et al., 2001 and Nagao et al., 2004).

We divided the ordinary coronal SPECT images into the anterior, middle and posterior regions. Anterior or posterior region was composed of the anterior or posterior half of the coronal SPECT slices (Fig. 1A). The middle region was composed of the middle one-third of the coronal SPECT slices. Then, middle region overlaps the posterior one-third slices of the anterior region and the anterior one-third slices of posterior region (Fig. 1B).
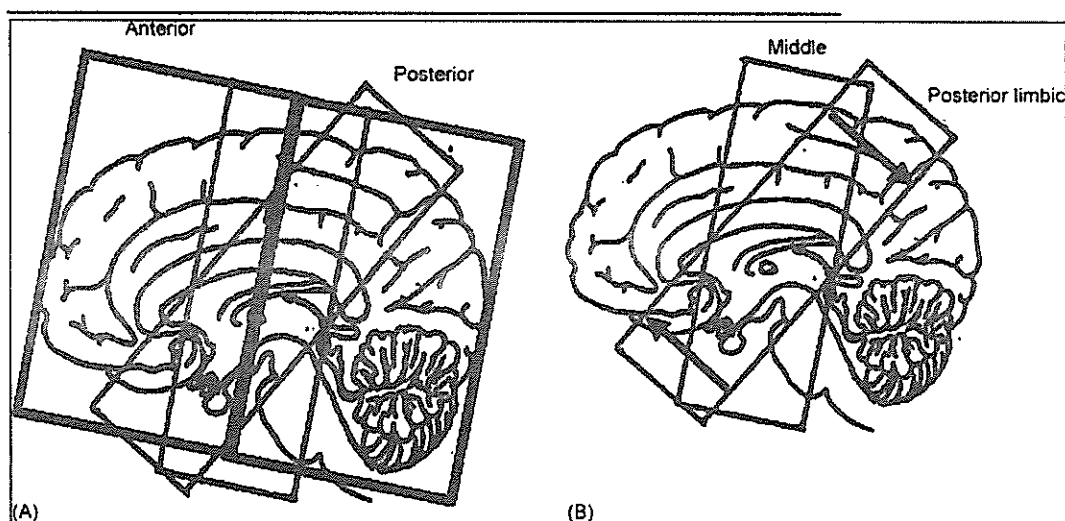

Fig. 1. (A) The schema of the anterior and posterior region indicates. Anterior and posterior regions comprised the anterior or posterior one-second of the coronal SPECT slices. (B) The schema of the middle region and the posterior limbic region indicates. The middle region comprised the middle one-third of the coronal SPECT slices. The posterior limbic region comprised the middle one-third slices that were reconstructed at 30° positive to the coronal plane.

The posterior limbic region was composed of the middle one-third slices that were reconstructed at 30° positive to the ordinary coronal plane (Fig. 1B). We calculated FD corresponding to anterior, middle, posterior and posterior limbic regions.

Computer selected the images that composed of each region automatically. The use of the images had no variation in reproducibility. In the all process of this analysis, the images were not transformed into a standard stereotactic space.

1.4. Statistical analysis

One-way analysis of variance with Bonferroni's correction was used to compare anterior FD, middle FD, posterior FD, posterior limbic FD and the ratio of posterior limbic FD to total FD among early AD, very early AD, and elderly control group. P value of less than 0.05 was considered statistically significant.

2. Results

Anterior FD for early AD, very early AD, and control groups were 1.20 ± 0.23, 1.19 ± 0.24, and 1.03 ± 0.19, respectively ($P = 0.006$ versus early AD group, $P = 0.02$ versus very early AD) (Fig. 2). There was no significant difference between early AD and very early AD groups.
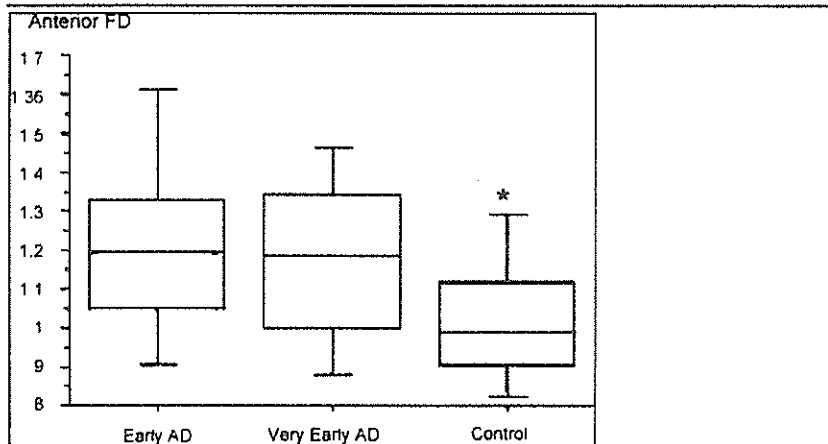

Fig. 2. The box-and-whisker plot shows anterior fractal dimension (FD) for patients with AD and elderly controls. The boxes represent 25–75% range with bisecting lines showing the median value, and the horizontal lines represent 10–90% range. $^{*}P = 0.006$ vs. early AD group, $P = 0.02$ vs. very early AD group.

Middle FD for early AD, very early AD, and control groups were 1.16 ± 0.24, 1.15 ± 0.27, and 0.96 ± 0.22 respectively ($P = 0.005$ versus early AD group, $P = 0.01$ versus very early AD) (Fig. 3). There was no significant difference between early AD and very early AD groups.
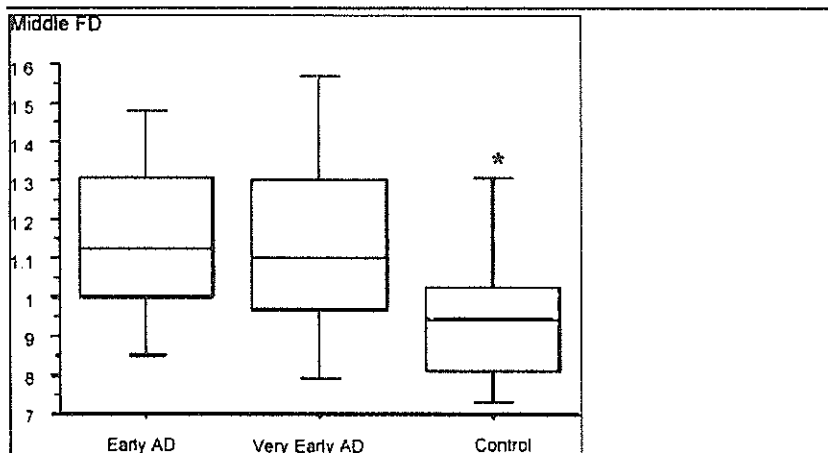

Fig. 3. The box-and-whisker plot shows middle fractal dimension (FD) for patients with AD and elderly controls. The boxes and the horizontal lines are same as in Fig. 2. $^{*}P = 0.005$ vs. early AD group, $P = 0.01$ vs. very early AD group.

216

Posterior FD for mild AD, very early AD, and control groups were 0.89 ± 0.18, 0.86 ± 0.18, and 0.74 ± 0.14 respectively ($P = 0.001$ versus early AD group, $P = 0.02$ versus very early AD group) (Fig. 4). There was no significant difference between early AD and very early AD groups.
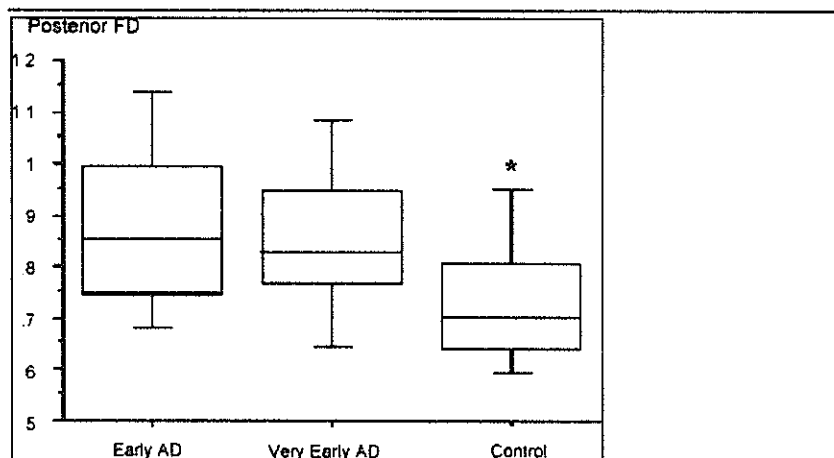

Fig. 4. The box-and-whisker plot shows posterior fractal dimension (FD) for patients with AD and elderly controls. The boxes and the horizontal lines are same as in Fig. 2. $^*P = 0.001$ vs. early AD group, $P = 0.02$ vs. very early AD group.

Posterior limbic FD for early AD, very early AD, and control groups were 1.03 ± 0.16, 1.02 ± 0.17, and 0.87 ± 0.14, respectively ($P = 0.001$ versus early AD group, $P = 0.001$ versus very early AD) (Fig. 5). There was no significant difference between early AD and very early AD groups.
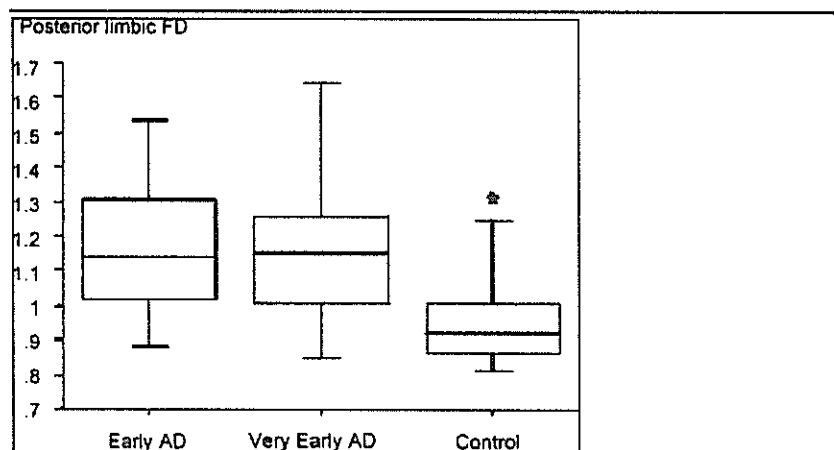

Fig. 5. The box-and-whisker plot shows posterior limbic fractal dimension (FD) for patients with AD and elderly controls. The boxes and the horizontal lines are same as in Fig. 2. $^*P = 0.001$ vs. mild AD group, $P = 0.001$ vs. very early AD group.

The ratio of posterior limbic FD to total FD for early AD, very early AD, and control groups was 1.13 ± 0.08, 1.16 ± 0.07, and 1.09 ± 0.07, respectively ($P = 0.0003$ versus very early AD). There was no significant difference between early AD and very early AD groups and between early AD and control groups. When patients with a posterior limbic FD of more than 0.96 and a posterior limbic FD to total FD ratio of more than 1.1 were diagnosed as having very early AD, these criteria separated very early AD patients from controls with a sensitivity of 76% (25/33) and a specificity of 81% (25/31) (Fig. 6).
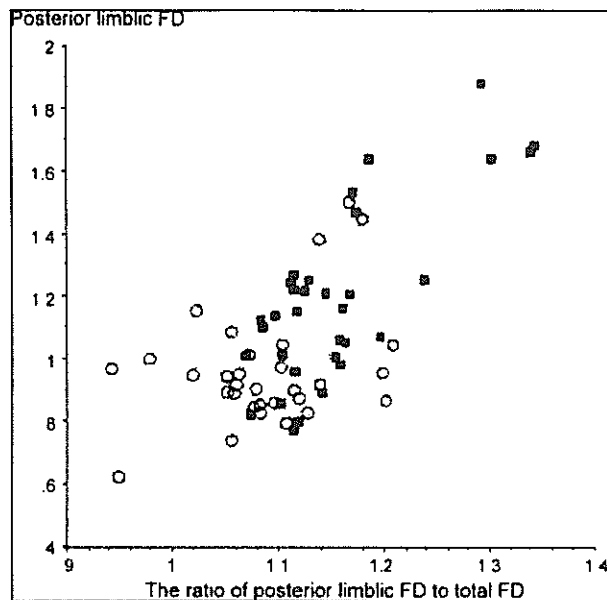
Fig. 6. Scatter plot of posterior limbic FD and the ratio of posterior limbic FD to total FD for 33 patients with very early AD (■) and 31 controls (○).

Representative SPECT images of very early AD are shown in Fig. 7. Fig. 7A is the coronal SPECT images, which show no definite hypoperfusion area. Fig. 7B is the SPECT images which are reconstructed at 30° positive to the coronal plane. Anterior FD, middle FD, posterior FD and posterior limbic FD of this very early case were 1.00, 0.98, 0.78, and 1.07.
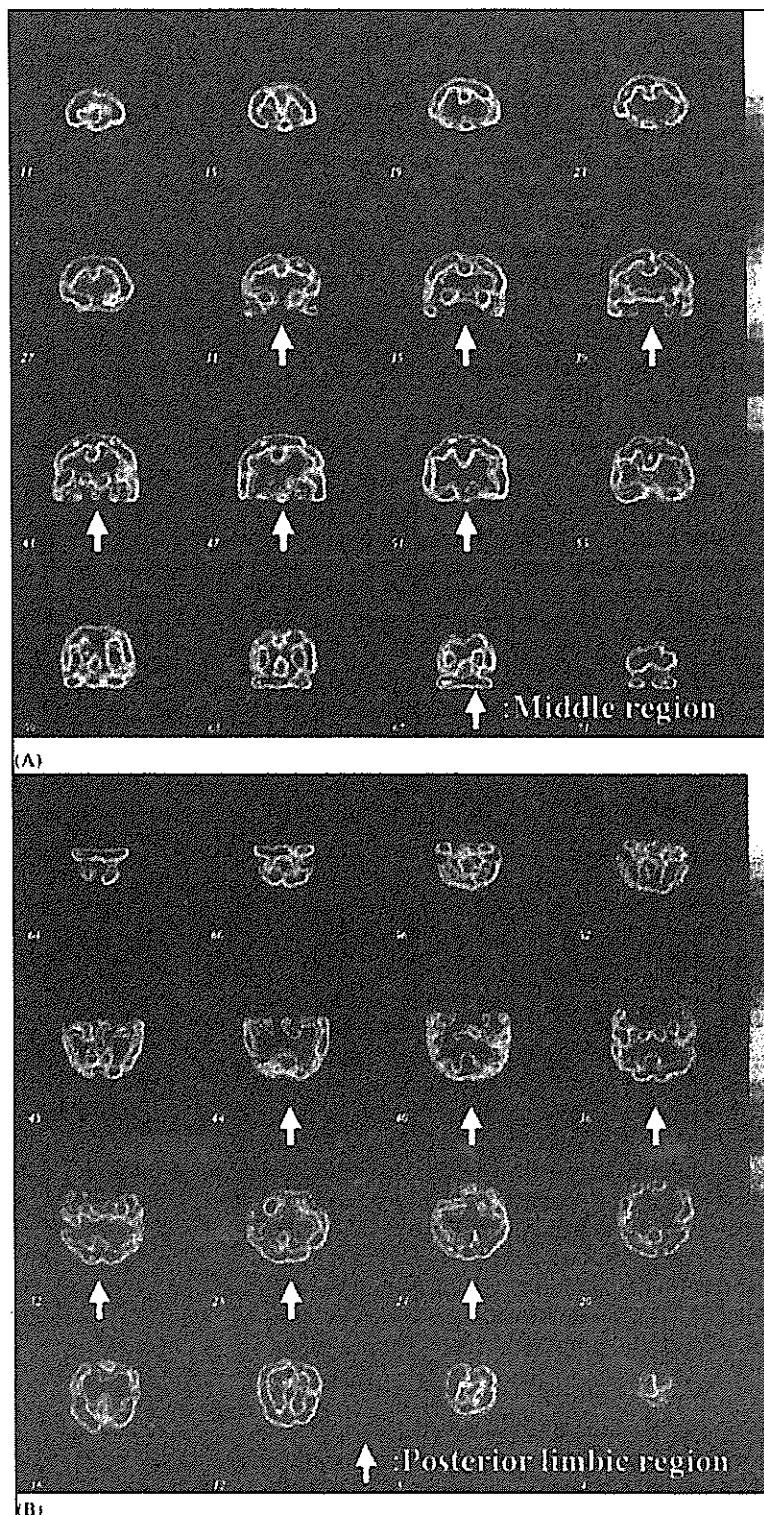
Fig. 7. (A) The coronal SPECT images for a 69-year-old female with very early Alzheimer's disease show no definite hypoperfusion area. The arrows indicate the slices corresponding to the middle region. Her anterior fractal dimension (FD), middle FD and posterior FD were 1.00, 0.98, and 0.78. (B) The SPECT images were reconstructed at 30° positive to the coronal plane, the same case as (A). The arrows indicate the slices corresponding to the posterior limbic region. Her posterior limbic FD was 1.07.

3. Discussion

219

In this study, 3D-FA allowed successful evaluation of the heterogeneous distribution of CBF SPECT in early stages of AD and healthy aging. There were significant differences in anterior FD, middle FD, posterior FD and posterior limbic FD between both (early and very early) AD groups and the normal control group. Of the four FDs, the most significant difference was found in the posterior limbic FD between very early AD and control groups. Although there was overlap in anterior FD, middle FD and posterior FD between the very early AD and control groups, criteria relating to both of the aforementioned parameters (a posterior limbic FD of more than 0.96 and a posterior limbic FD to total FD ratio of more than 1.1) clearly distinguished very early AD patients from elderly controls. The ratio of posterior limbic FD to total FD indicates the predominance of the heterogeneity of the posterior limbic perfusion in the whole CBF distribution. These results suggest that the heterogeneity of posterior limbic perfusion may be the reliable imaging marker for predicting the clinical severity at the mild stage of AD.

The posterior limbic region added the anterior temporal lobe to the middle region and excluded the primary motor cortex in parietal lobe from the middle region, since the posterior limbic images were reconstructed at 30° positive to the ordinary coronal plane (Fig. 1). Furthermore, the posterior limbic region excluded the occipital lobe and cerebellum from the posterior region (Fig. 1). Thus, the posterior limbic region included the hippocampal amygdaloid complex, thalamus, a part of anterior cingulate cortex, posterior cingulate cortex and precuneus, in which were seen slight hypoperfusion at early stage of AD (Minoshima et al., 1997 and Johnson et al., 1998). In ordinary transaxial or coronal images, the hippocampus, posterior cingulate cortex and precuneus are divided into several parts and shown on several separate slices. As a result, it was difficult to evaluate blood flow of the small part in each slice. On the other hand, the posterior limbic images became nearly parallel to the long axis of the hypocampal formation, posterior cingulate cortex and precuneus and could demonstrate slight reduced CBF in these regions. Consequently, CBF distribution on posterior limbic region may be more heterogeneous than that on the other regions.

In addition, this result is consistent with recent studies of mild cognitive impairment (MCI), the amnesic prodrome of AD, using SPECT or PET. Since the seminal findings of Minoshima et al., 1994 and Minoshima et al., 1997 of posterior cingulate and adjacent cingulo-parietal hypometabolism in mild stage AD, SPECT hypoperfusion in this region has been identified in MCI cases that subsequently converted to AD (Johnson et al., 1998 and Kogure et al., 2000). Furthermore, posterior cingulate and adjacent cingulo-parietal hypometabolism was identified in MCI cases (Nestor et al., 2003) and such changes were reported as a predictor of early conversion from MCI to AD (Chetelat et al., 2003). We experienced five stable MCI patients with a follow up period of more than 3 years. Their posterior limbic FD (mean: 0.89) is almost equal to that for controls when CBF SPECT was performed with the same protocol. Posterior limbic FD has possibility to be a predictor of conversion from MCI to AD. Maruyama et al. reported that increased level of the cerebrospinal fluid (CSF)-tau might help in detecting MCI subjects who are predicted to develop AD (Maruyama et al., 2001). However, we did not have CSF data from the patients enrolled in the present study. The comparison of FD with the biochemical assays in terms of accuracy of discrimination between normal subjects and probable AD or AD-converted MCI is a theme in the future studies.

The recent development of computer assisted analysis using three-dimensional stereotactic surface projections (3D-SSP) afforded more objective and more reliable assessment than the visual inspection of the standard transaxial images. Imabayashi et al. reported 3D-SSP demonstrated a high accuracy of 86% for discriminating patients with AD at a very early stage from control subjects (Imabayashi et al., 2004). 3D-FA is a simple and objective image analysis method and does not use a standard stereotactic space or a statistical image technique such as 3D-SSP. Although a methodology of 3D-FA is different from 3D-SSP, 3D-FA resulted in a high accuracy for discriminating very early AD patients from controls. We expect that combination of 3D-FA with 3D-SSP may increase the diagnostic accuracy for early AD.

Age-related and regional decreases in CBF have been reported in many studies. In recent PET studies, bilateral and symmetrically distributed effects of age were most marked in the

inferior and posterior lateral frontal, anterior cingulate, perisylvian temporo-parietal and anterior temporal cortices, and, left caudate and anterior thalamus. However, the anterior dorsolateral prefrontal regions, posterior cingulate, precuneus, some occipital association and inferior occipito-temporal cortices, as well as other areas, were relatively less affected, while no significant effects of aging were identified in most of the occipital cortex (Mozley et al., 1997, Kuhl et al., 1982, Moeller et al., 1996 and Petit-Taboue et al., 1998). Relative hypofrontality with increased age and the lesser effects of age on the posterior brain are consistent findings of most previous studies. Due to the age-related decrease in anterior CBF, there might be unacceptably high overlap in the anterior FD between AD patients and controls.

In conclusion, 3D-FA indicated significant differences in the heterogeneity of CBF distribution between patients with very mild stage AD and healthy elderly. Posterior limbic FD that indicates the heterogeneity of this region may be useful for objectively distinguishing patients with very early AD and MCI from healthy elderly.

Acknowledgments

References

Aftanas and Royce, 1969 M.S. Aftanas and J.R. Royce, A factor analysis of brain damage tests administered to normal subjects with factor score comparisons across ages, *Multivar. Behav. Res.* 4 (1969), pp. 459–481. **Full Text** via CrossRef

Chetelat et al., 2003 G. Chetelat, B. Desgranges, V. de la Sayette, F. Viader, F. Eustache and J.C. Baron, Mild cognitive impairment Can FDG-PET predict who is to rapidly convert to Alzheimer's disease, *Neurology* **60** (2003), pp. 1374–1377. Abstract + References in Scopus | Cited By in Scopus

Cummings et al., 1994 J.L. Cummings, M. Mega, K. Gray, S. Rosenberg-Thompson, D.A. Carusi and J. Gornbein, The neuropsychiatric inventory: comprehensive assessment of psychopathology in dementia, *Neurology* **44** (1994), pp. 2308–2314. Abstract + References in Scopus | Cited By in Scopus

Drayer, 1988 B.P. Drayer, Imaging of the aging brain. Part 1. Normal findings, *Radiology* **166** (1988), pp. 785–796. Abstract + References in Scopus | Cited By in Scopus

Folstein et al., 1975 M.F. Folstein, S.E. Folstein and P.R. McHugh, Mini-mental state: a practical method for grading the cognitive state of patients for clinician, *J. Psychiat. Res.* **12** (1975), pp. 189–198. Abstract | Abstract + References in Scopus | Cited By in Scopus

Foster et al., 1984 N.L. Foster, T. Chase, L. Mansi, R. Brooks, P. Fedio, N.J. Patronas and G. Di Chiro, Cortical abnormalities in Alzheimer's disease, *Ann. Neurol.* **16** (1984), pp. 649–654. **Full Text** via CrossRef | Abstract + References in Scopus | Cited By in Scopus

Haxby et al., 1985 J. Haxby, R. Duara, C. Grandy, N. Cutler and S. Rapaport, Relations between neuropsychological and cerebral metabolic asymmetries in early Alzheimer's disease, *J. Cereb. Blood Flow Metab.* **5** (1985), pp. 193–200. Abstract + References in Scopus | Cited By in Scopus

Holman et al., 1992 B.L. Holman, K.A. Johnson, G. Basem, P. Carvalho and A. Satlin, The scintigraphic appearance of Alzheimer's disease: a prospective study using Tc-99m HMPAO

SPECT, *J. Nucl. Med.* **33** (1992), pp. 181–185. Abstract + References in Scopus | Cited By in Scopus

Imabayashi et al., 2004 E. Imabayashi, H. Matsuda, T. Asada, T. Ohnishi, S. Sakamoto, S. Nakano and T. Inoue, Superiority of 3-dimensional stereotactic surface projection analysis over visual inspection in discrimination of patients with very early Alzheimer's disease from controls using brain perfusion SPECT, *J. Nucl. Med.* **45** (2004), pp. 1450–1457. Abstract + References in Scopus | Cited By in Scopus

Johnson et al., 1998 K.A. Johnson, K. Jones, B.L. Holman, J.A. Becker, P.A. Spiers, A. Satlin and M.S. Alber, Preclinical prediction of Alzheimer's disease using SPECT, *Neurology* **50** (1998), pp. 1563–1571. Abstract + References in Scopus | Cited By in Scopus

Kogure et al., 2000 D. Kogure, H. Matsuda, T. Ohnishi, T. Ohnishi, T. Asada, M. Uno, T. Kunihiro, S. Nakano and M. Takasaki, Longitudinal evaluation of early Alzheimer's disease using brain perfusion SPECT, *J. Nucl. Med.* **41** (2000), pp. 1155–1162.

Kokmen et al., 1993 E. Kokmen, C.M. Beard, P.C. O'Brien, K. Offord and L.T. Kurland, Is the incidence of dementing illness changing? A 25-year time-trend study in Rochester, MN (1960–1984), *Neurology* **43** (1993), pp. 1887–1892. Abstract + References in Scopus | Cited By in Scopus

Kuhl et al., 1982 D.E. Kuhl, E.J. Metter, W.H. Riege and M.E. Phelps, Effects of human aging on patterns of local cerebral glucose utilization determined by the [18F] fluorodeoxyglucose method, *J. Cereb. Blood Flow Metab.* **2** (1982), pp. 163–171. Abstract + References in Scopus | Cited By in Scopus

Lawton and Brody, 1969 M.P. Lawton and E.M. Brody, Assessment of older people: self-maintaning and instrumental activities of daily living, *Gerontologist* **9** (1969), pp. 179–186. Abstract + References in Scopus | Cited By in Scopus

Mandelbrot, 1967 B. Mandelbrot, How long is the coast of Britain? Statistical self-similarity and fractal dimension, *Science* **156** (1967), pp. 636–638. Abstract + References in Scopus | Cited By in Scopus

Maruyama et al., 2001 M. Maruyama, H. Arai, M. Sugita, H. Tanji, M. Higuchi, N. Okamura, T. Matsui, S. Higuchi, S. Matsushita, H. Yoshida and H. Sasaki, Cerebrospinal fluid amyloid beta (1-42) levels in the mild cognitive impairment stage of Alzheimer's disease, *Exp. Neurol.* **172** (2001), pp. 433–436. Abstract | **Abstract + References** | PDF (58 K) | Abstract + References in Scopus | Cited By in Scopus

McKhann et al., 1984 G. McKhann, D. Drachman, M. Folstein, R. Katzman, D. Price and E.M. Stadlan, Clinical diagnosis of Alzheimer's disease: report of the NINCDS-ADRDA Work Group under the auspices of Department of Health and Human Services Task Force on Alzheimer's Disease, *Neurology* **34** (1984), pp. 939–944. Abstract + References in Scopus | Cited By in Scopus

Messa et al., 1994 C. Messa, D. Perani, G. Lucignani, A. Zenorini, F. Zito, G. Rizzo, F. Grassi, A. Del Sole, M. Franceschi and M.C. Gilardi, High-resolution technetium-99m HMPAO SPECT in patients with probable Alzheimer's disease: comparison with fluorine-18-FDG-PET, *J. Nucl. Med.* **35** (1994), pp. 210–216. Abstract + References in Scopus | Cited By in Scopus

Minoshima et al., 1994 S. Minoshima, N.L. Foster and D.E. Kuhl, Posterior cingulate cortex in Alzheimer's disease, *Lancet* **344** (1994), p. 895. Abstract | Abstract + References in Scopus | Cited By in Scopus

Minoshima et al., 1997 S. Minoshima, B. Giordani, S. Berent, K.A. Frey, N.L. Foster and D.E. Kuhl, Metabolic reduction in the posterior cingulate cortex in very early Alzheimer's disease, *Ann. Neurol.* **42** (1997), pp. 85–94. **Full Text** via CrossRef | Abstract + References in Scopus | Cited By in Scopus

Moeller et al., 1996 J.R. Moeller, T. Ishikawa, V. Dhawan, P. Spetsieris, F. Mandel, G.E.

222

Alexander, C. Grandy, P. Pietrini and D. Eidelberg, The metabolic topography of normal aging, *J. Cereb. Blood Flow Metab.* **16** (1996), pp. 385–398. **Full Text** via CrossRef | Abstract + References in Scopus | Cited By in Scopus

Mohs et al., 1983 R.C. Mohs, W.G. Rosen and K.L. Davis, The Alzheimer's disease assessment scale: an instrument for assessing treatment efficacy, *Psychopharmacol. Bull.* **19** (1983), pp. 448–450. Abstract + References in Scopus | Cited By in Scopus

Morris, 1993 J.C. Morris, The clinical dementia rating (CDR): current version and screening rules, *Neurology* **43** (1993), pp. 2412–2414. Abstract + References in Scopus | Cited By in Scopus

Mozley et al., 1997 P.D. Mozley, A.M. Sadek, A. Alavi, R.C. Gur, L.R. Muenz, B.J. Bunow, H.J. Kim, M.H. Stecker, P. Jolles and A. Newberg, Effects of aging on the cerebral distribution of technetium-99m hexamethylpropylene amine oxime in healthy humans, *Eur. J. Nucl. Med.* **24** (1997), pp. 754–761. **Full Text** via CrossRef | Abstract + References in Scopus | Cited By in Scopus

Nagao et al., 2001 M. Nagao, K. Murase, T. Kikuchi, M. Ikeda, A. Nebu, R. Fukuhawa, Y. Sugawara, H. Miki and J. Ikezoe, Fractal analysis of cerebral blood flow distribution in Alzheimer's disease, *J. Nucl. Med.* **42** (2001), pp. 1445–1450.

Nagao and Murase, 2002 M. Nagao and K. Murase, Measurement of heterogeneous distribution on Technegas SPECT images by three-dimensional fractal analysis, *Ann. Nucl. Med.* **16** (2002), pp. 369–376. Abstract + References in Scopus | Cited By in Scopus

Nagao et al., 2004 M. Nagao, Y. Sugawara, M. Ikeda, R. Fukuhara, K. Hokoishi, K. Murase, T. Mochizuki, H. Miki and T. Kikuchi, Heterogeneity of cerebral blood flow in frontotemporal lobar degeneration and Alzheimer's disease, *Eur. J. Nucl. Med.* **31** (2004), pp. 162–168. **Full Text** via CrossRef | Abstract + References in Scopus | Cited By in Scopus

Nebu et al., 2001 A. Nebu, M. Ikeda, R. Fukuhara, K. Shigenobu, N. Maki, K. Hokoishi, K. Komori, T. Yasuoka and H. Tanabe, Relationship between blood flow kinetics and severity of Alzheimer's disease: assessment of severity using a questionnaire-type examination, Alzheimer's disease assessment scale, cognitive sub-scale (ADAScog), *Dement. Geriatr. Cogn. Disord.* **12** (2001), pp. 318–325. **Full Text** via CrossRef | Abstract + References in Scopus | Cited By in Scopus

Nelson, 1990 T. Nelson, Fractal physiologic complexity, scaling, and opportunities for imaging, *Invest. Radiol.* **25** (1990), pp. 1140–1148. Abstract + References in Scopus | Cited By in Scopus

Nestor et al., 2003 P.J. Nestor, T.D. Fryer, P. Smielewski and J.R. Hodges, Limbic hypometabolism in Alzheimer's disease and mild cognitive impairment, *Ann. Neurol.* **54** (2003), pp. 343–351. **Full Text** via CrossRef | Abstract + References in Scopus | Cited By in Scopus

Petersen et al., 1994 R.C. Petersen, G.E. Smith, R.J. Ivnik, E. Kokmen and E.G. Tangalos, Memory function in very early Alzheimer's disease, *Neurology* **44** (1994), pp. 867–872. Abstract + References in Scopus | Cited By in Scopus

Petit-Taboue et al., 1998 M.C. Petit-Taboue, B. Landeau, J.F. Desson, B. Desgranges and J.C. Baron, Effects of healthy aging on the regional cerebral metabolic rate of glucose assessed with statistical parametric mapping, *Neuroimage* **7** (1998), pp. 176–184. Abstract | **Abstract + References** | PDF (413 K) | Abstract + References in Scopus | Cited By in Scopus

Yoshikawa et al., 2003a T. Yoshikawa, K. Murase, N. Oku, K. Kitagawa, M. Imaizumi, M. Takasawa, P. Rishu, K. Hashikawa, T. Nishikawa, M. Hori and M. Matsumoto, Quantification of the heterogeneity of cerebral blood flow in vascular dementia, *J. Neurol.* **250** (2003), pp. 194–200. **Full Text** via CrossRef | Abstract + References in Scopus | Cited By in Scopus

223

Yoshikawa et al., 2003b T. Yoshikawa, K. Murase, N. Oku, K. Kitagawa, M. Imaizumi, M. Takasawa, T. Nishikawa, M. Matsumoto, J. Hatazawa and M. Hori, Statistical image analysis of cerebral blood flow in vascular dementia with small-vessels disease, *J. Nucl. Med.* 44 (2003), pp. 505–511. Abstract + References in Scopus | Cited By in Scopus

Corresponding author at: Department of Radiology, Ehime Prefectural Imabari Hospital, Ishii-cho 4-5-5, Imabari-city, Ehime 794-0006, Japan. Tel.: +81 89 832 7111; fax: +81 89 822 1398.

This Document
- SummaryPlus
- ▶ **Full Text + Links**
  - ·Thumbnail Images
- PDF (266 K)

Actions
- Cited By
- Save as Citation Alert
- E-mail Article
- Export Citation
- Add to my Quick Links

CT-guided needle biopsy of lung lesions: A survey of severe complication based on 9783 biopsies in Japan

Noriyuki Tomiyama[a,] , Yoshifumi Yasuhara[b], Yasuo Nakajima[c], Shuji Adachi[d], Yasuaki Arai[e],
Masahiko Kusumoto[e], Kenji Eguchi[f], Keiko Kuriyama[g], Fumikazu Sakai[h], Masayuki Noguchi[i],
Kiyoshi Murata[j], Sadayuki Murayama[k], Teruhito Mochizuki[l], Kiyoshi Mori[m], Kozo Yamada[n]

[a] Department of Radiology, Osaka University Graduated School of Medicine, 2-2 Yamadaoka, Suita, Osaka 565-0871, Japan
[b] Department of Radiology, National Hospital Organization Ehime National Hospital, Japan
[c] Department of Radiology, St. Marianna University School of Medicine, Japan
[d] Department of Radiology, Hyogo Medical Center for Adults, Japan
[e] Department of Diagnostic Radiology, National Cancer Center, Japan
[f] Department of Oncology, Tokai University School of Medicine, Japan
[g] Department of Radiology, Kinki Central Hospital of the Mutual Aid Association of Public School Teachers, Japan
[h] Department of Radiology, Tokyo Metropolitan Komagome Hospital, Japan
[i] Department of Pathology, Graduate School of Comprehensive Human Sciences, Institute of Basic Medical Sciences, University of Tsukuba, Japan
[j] Department of Radiology, Shiga University of Medical Science, Japan
[k] Faculty of Medicine, University of the Ryukyus, Japan
[l] Department of Radiology, Ehime University School of Medicine, Japan
[m] Department of Thoracic Oncology, Tochigi Cancer Center, Japan
[n] Department of Thoracic Oncology, Kanagawa Cancer Center, Japan

Received 3 November 2005; received in revised form 4 February 2006; accepted 6 February 2006

Abstract

Purpose: The aim of our study was to update the rate of severe complications following CT-guided needle biopsy in Japan via a mailed survey.

Materials and methods: Postal questionnaires regarding CT-guided needle biopsy were sent out to multiple hospitals in Japan. The questions regarded: the total number and duration of CT-guided lung biopsies performed at each hospital, and the complication rates and numbers of pneumothorax, hemothorax, air embolism, tumor seeding, tension pneumothorax and other rare complications. Each severe complication was followed with additional questions.

Results: Data from 9783 biopsies was collected from 124 centers. Pneumothorax was the most common complication, and occurred in 2412 (35%) of 6881 cases. A total of 39 (35%) hospitals reported 74 (0.75%) cases with severe complications. There were six cases (0.061%) with air embolism, six cases (0.061%) with tumor seeding at the site of the biopsy route, 10 cases (0.10%) with tension pneumothorax, six cases (0.061%) with severe pulmonary hemorrhage or hemoptysis, nine cases (0.092%) with hemothorax, and 27 cases (0.26%) with others, including heart arrest, shock, and respiratory arrest. From a total of 62 patients with severe complications, 54 patients (0.55%) recovered without sequela, however one patient (0.01%) recovered with hemiplegia due to cerebral infarction, and the remaining seven patients (0.07%) died.

Conclusions: This is the first national study documenting severe complications with respect to CT-guided needle biopsy in Japan. The complication rate in Japan is comparable to internationally published figures. We believe this data will improve both clinicians as well as patients understanding of the risk versus benefit of CT-guided needle biopsy, resulting better decisions.

© 2006 Elsevier Ireland Ltd. All rights reserved.

Keywords: CT-guided needle biopsy; Complication; Lung nodule

Corresponding author. Tel.: +81 6 6879 3434; fax: +81 6 6879 3439.
E-mail address: tomiyama@radiol.med.osaka-u.ac.jp (N. Tomiyama).

1. Introduction

Transthoracic needle biopsy is a common procedure used mainly to elucidate the nature of pulmonary nodules [1,2]. CT has rapidly become the guidance modality of choice for performing transthoracic needle biopsy due to technical advances in CT and its better detection of pulmonary lesions, which sometimes cannot be identified on chest radiograph [3].

CT-guided needle biopsy is generally regarded as a safe procedure, although pneumothorax and other rare complications can sometimes occur [4]. There have been occasional reports of deaths due to severe complications, such as, air embolism following lung biopsy [5]. Fortunately, these complications are generally very rare; previously published data shows wide variations in complication rates, making them difficult to generalize [5–8].

The aim of our study was to update the rate of severe complications following CT-guided needle biopsy in Japan via a mailed survey.

2. Materials and methods

Postal questionnaires regarding CT-guided needle biopsy were sent out to named radiologists at 101 university hospitals and cancer centers in Japan in August 2001. The radiologists at these hospitals were asked to pass duplications of the questions to other associate hospitals. The questions required information regarding: the total number and duration of CT-guided lung biopsies performed at each hospital, and the complication rates, numbers of pneumothorax, hemothorax, air embolism, tumor seeding, tension pneumothorax, severe pulmonary hemorrhage or hemoptysis which was treated with drugs for hemostasis and other rare complications, and mortalities and morbidities after that.

We defined a case as having a severe complication when one of the following criteria was met: (1) the duration of hospital stay was prolonged due to the biopsy, (2) a special technique or treatment was required to treat the complication, (3) a special procedure was required for resuscitation, and (4) shock or pre-shock developed. Each severe complication was followed with additional questions, including diagnosis of the complication, the position of the pulmonary lesion, the distance of the pulmonary lesion from the peripheral pleura, whether the lesion was located near the hilum or large pulmonary vessel, whether there was any reasonable factor causing the complication such as cough during biopsy, biopsy technique (CT-fluoroscopy or Co-axial method), the number of biopsies for each case, type and size of the needle, and presence of significant sequela from the complication.

Furthermore, the questionnaire included the following enquiries: whether emergency medication was prepared for resuscitation in the operating room, whether the patient was treated by the intravenous route and monitors, such as automatic sphygmomanometer, pulse oximetry, and electrocar-

diography. Finally, availability of access to other departments in case of emergency was questioned. Postal replies of questionnaire had been received for a year, and these answers were analyzed.

3. Results

A total of 9783 biopsy data were collected from 124 centers. The average number of biopsies performed per center was 79 cases, and that per center per year was 21 cases. The number of institutions in which hyperbaric oxygen recompression can be performed was 41 of 114 (37%) hospitals. Patients were kept on peripheral intravenous drip infusion in 86 of 92 (93%) hospitals, automatic sphygmomanometer in 38 of 92 (41%) hospitals, pulse oximetry in 32 of 92 (35%) hospitals, and electrocardiography in 8 of 92 (9%) hospitals.

Pneumothorax was the most common complication, and occurred in 2412 (35%) of 6881 cases. The number of centers that reported severe complications was 39 (35%) of 114 centers. The total number of overall severe complications was 74 (0.75%) cases. Of these, details of the complications in 64 cases are described in Table 1. There were six cases (0.061%) with air embolism, six cases (0.061%) with tumor seeding at the site of the biopsy route, 10 cases (0.10%) with tension pneumothorax, six cases (0.061%) with severe pulmonary hemorrhage or hemoptysis, 10 cases (0.10%) with hemothorax, and 26 cases (0.26%) with others. The others included 14 cases of pneumothorax requiring temporal drainage of the pneumothorax or chest tube insertion, three cases of heart arrest, and so on. There was no report of coughing during needle placement into the thorax in any of the cases with air embolism. Two of six pulmonary lesions were complicated with air emboli located near the large pulmonary vessel, and one lesion contained a cavity (Table 2). Tumor seeding occurred in two cases following CT-guided biopsy performed

Table 1
Summary of 64 cases of severe complications

Severe complications	No.
Pneumothorax requiring drainage of air	14
Tension pneumothorax	10
Hemothorax	10
Air embolism	6
Tumor seeding	6
Pulmonary hemorrhage of hemoptysis	6
Heart arrest	3
Respiratory arrest	1
Shock	1
Cyanosis	1
Cardiac tamponade	1
Pneumomediastinum	1
Mediastinal hematoma	1
Loss of consciousness	1
Severe pain of biopsied site	1
disseminated intravascular coagulation (DIC)	1
Total	64

Table 2
Summary of cases of air embolism

No.	Age	Sex	Size (mm)	Location (lobe)	Distance from pleura (mm)	Large vessel near the nodule	Cavity	CT-fluoloscopy	Co-axial method	No. of biopsy	Technique of biopsy	Size of the needle	Sequela
1	72	F	20	Left lower	40	Yes	No	Yes	No	2	Core biopsy	18G	Death
2	59	M	10	Left lower	20	No	No	NA[a]	Yes	1	Core biopsy	18G	Totally improved
3	57	F	7	Right middle	25	No	No	Yes	No	1	Core biopsy	18G	Totally improved
4	74	M	20	Right upper	25	Yes	No	Yes	No	2	Core biopsy	20G	Partially improved
5	57	M	12	Right lower	3	No	No	No	Yes	1	Core biopsy	20G	Totally improved
6	75	M	25	Right lower	18	No	Yes	No	No	1	Core biopsy	18G	Totally improved

[a] NA, information was not available.

by the Co-axial method (Table 3). In one of these two cases, the tip of the outer cannula was placed within the chest wall, so that seeding obviously occurred by direct contact of the inner needle with the biopsy route.

From a total of 62 cases with severe complications, 54 cases (0.55%) were recovered without sequela, and one case (0.01%) recovered but with hemiplegia due to cerebral infarction. Unfortunately, four (0.04%) of the remaining seven cases died just after the CT-guided biopsy procedure; these consisted of one case of air embolism, one case of DIC, and two cases of heart arrest. Three cases (0.03%) of the remaining seven cases died several years later due to tumor seeding. Four cases complicated with air embolism, three of which were treated with hyperbaric oxygen recompression, were recovered without sequela out of a total of six cases. In 23 (50%) of 46 centers, an emergency team was able to attend when a severe complication occurred.

4. Discussion

Recently, many small pulmonary lesions, which cannot be detected on chest radiograph, have been easily visualized by CT examination in daily clinical work. These lesions are usually followed with CT, or in some cases these are biopsies using CT-guided technique. CT-guided needle biopsy is a widely accepted technique and is one of the principal methods for evaluating a pulmonary lesion [9]. Although it is not rare to have minor complications due to CT-guided needle biopsy, such as, a small amount of pneumothorax and pulmonary hemorrhage, these complications improve without any treatment [5]. On the other hand, it is well known that potentially life-threatening complications such as air embolism and tumor seeding can occur. Fortunately, the frequency of these complications is considered very rare [5]. However, the number of published reports has shown that the incidence of air embolism has been increasing over the last several years. Only seven cases with air embolism were documented in the 20 years before 1995 [10–16], whereas six cases have already been published in the last 10 years [17–22].

This is the first national research study demonstrating the incidence rate of severe complications with respect to CT-guided needle biopsy based on a large number of biopsy cases using a multi-center survey.

The most common complication of transthoracic percutaneous needle biopsy is pneumothorax, with a frequency rate of 0–61%, whereas the incidence of pneumothorax requiring chest tube drainage ranges from 1.6% to 17% [23]. In the present study, the rate of pneumothorax was 35.1%, which is considered comparable to the previous studies.

Sinner's review of the literature determined that there were two cases suspected of air embolism in 2726 patients [5]. He estimated that the relative risk of air embolism per patient was about 0.07%. In the present study of 9783 biopsies, air embolism occurred in six patients, resulting in an incidence

Table 3
Summary of cases of tumor seeding

No.	Age	Sex	Size (mm)	Location	Distance from pleura (mm)	Co-axial method	No. of biopsy	Technique of biopsy	Size of the needle
1	72	M	30	Right upper	0	No	1	Core biopsy	18G
2	73	M	30	Left lower	30	Yes	3	Core biopsy	18G
3	71	M	10	Right upper	20	No	2	Aspiration biopsy	22G
4	30	F	28	Left upper	76	No	2	Core biopsy	18G
5	69	M	15	Right lower	0	No	2	Core biopsy	21G
6	77	M	12	Right upper	30	Yes	2	Core biopsy	20G

rate of 0.06%, which also shows no major difference from the previously reported complication rate. However, in the present study, there were several cases of severe complications including cardiac and respiratory arrest, and shock, which can be secondary to air embolism, although it is very difficult to confirm air embolism in the coronary artery in cases of myocardial infarction when the patient has not been scanned at the level of the heart. It is speculated that concurrent cough during the procedure has a high possibility of an air embolism misplacing the biopsy needle into the large vessel adjacent to the pulmonary lesion. Among the total of six cases with air emboli in the present study, two cases demonstrated biopsied pulmonary lesions located close to the large vessels, however the remaining four cases have no close relation to the large vessels. There were no reports of coughing during the procedure in any of the cases complicated by air embolism. Air embolism even occurred in a case in which the nodule was very near the pleura (case no. 5). In our study, all cases with air emboli had undergone CT-guided biopsy using a core biopsy needle of 18–20 gauge, which is greater in diameter than the usually used fine aspiration needles. Having said that, in the previous reviews, most cases with air emboli were biopsied by fine aspiration needles, and there are two prior reports of air embolism following CT-guided lung needle marking using thin needles without recent biopsy [24–26].

Tumor seeding into the needle tract seems to be a rare possibility in several case reports [27–34]. There were six cases (0.06%) of tumor seeding in our study, which is a relatively high frequency compared to previous studies [5,35]. The true incidence of tumor seeding along the needle may be underestimated as not all cases can be diagnosed, and many patients die before these metastases become clinically apparent. Tumor seeding appears to depend on the size of the needle, therefore large-bore needles carry a relatively greater risk of tumor seeding, however tumor seeding following a fine needle aspiration was reported in one case of our study. It is thought that CT-guided biopsy performed using the Co-axial method has less frequency of tumor seeding as the outer cannula minimizes direct contact of the tumor cells with the biopsy route. Surprisingly, tumor seeding occurred in two cases using the Co-axial method. We speculate that the outer cannula was not appropriately placed.

Unfortunately, there were seven patients (0.07%) who died in our study due to complications in the CT-guided needle biopsy. Greene [6] estimated the mortality rate associated with fine needle aspiration to be 0.02%, how-

ever Richardson et al. [8] reported eight deaths (0.15%) in their study due to complications in CT-guided needle biopsy. Most of the deaths in the present study were attributed to fatal air embolism. Three cases of air embolism that were treated with hyperbaric oxygen recompression were recovered without sequela, which may suggest hyperbaric oxygen recompression therapy is effective for treatment of air embolism, and for reducing the mortality rate.

Our study has several limitations, including selection bias, the long period of the study, multi-center analysis with a large variety of techniques and CT scanners, and the possibility of missing or misdiagnosing significant complications such as the number of air emboli and tumor seeding. Moreover, our study is a retrospective questionnaire-based analysis rather than a prospective survey.

In conclusion, this is the first nation-wide study documenting severe complications with respect to CT-guided needle biopsy in Japan. The complication rate in Japan is comparable to internationally published figures. We believe this data will improve both clinicians as well as patients understanding of the risk versus benefit of CT-guided needle biopsy, resulting better decisions.

References

[1] Sinner WN. Pulmonary neoplasms diagnosed with transthoracic needle biopsy. Cancer 1979;43:1533–40.

[2] Klein JS, Zarka MA. Transthoracic needle biopsy. J Thorac Imag 1997;12:232–49.

[3] Hirose T, Mori K, Machida S, et al. Computed tomographic fluoroscopy-guided transthoracic needle biopsy for diagnosis of pulmonary nodules. Jpn J Clin Oncol 2000;30:259–62.

[4] Berquist TH, Bailey PB, Cortese DA, et al. Transthoracic needle biopsy: accuracy and complication in relation to location and type of lesion. Mayo Clin Proc 1980;55:475–81.

[5] Sinner WN. Complications of percutaneous transthoracic needle aspiration biopsy. Acta Radiol Diag 1976;17:813–28.

[6] Greene RE. Transthoracic needle aspiration biopsy. In: Athanasoulis CA, Pfister RC, Greene RE, Robertson GH, editors. Interventional radiology. Pliladelphia: Sanders; 1982. p. 587–634.

[7] Klein JS, Zarka MA. Transthoracic needle biopsy. Radiol Clin North Am 2000;38:235–66.

[8] Richardson CM, Pointon KS, Manhire AR, et al. Percutaneous lung biopsies: a survey of UK practice based on 5444 biopsies. Br J Radiol 2002;75:731–5.

[9] Belfiore G, Filippo SD, Guida C, et al. CT-guided needle biopsy of lesions. Nucle Med Biol 1994;21:713–9.

[10] Wescott JL. Air embolism complicating percutaneous needle biopsy of the lung. Chest 1973;63. pp. 108–108.

[11] Aberle DR, Gamsu G, Golden JA. Fatal systemic arterial air embolism following lung needle aspiration. Radiology 1987;165:351–3.

[12] Cianci P, Posin JP, Shimshak RR, et al. Air embolism complicating percutaneous thin needle biopsy of lung. Chest 1987;92:749–50.

[13] Tolly TL, Feldmeier JE, Czarnecki D. Air embolism complicating percutaneous lung biopsy. AJR Am J Roentgenol 1988;150:555–6.

[14] Baker BK, Awwad EE. Computed tomography of fatal cerebral air embolism following percutaneous aspiration biopsy of the lung. JCAT 1988;12:1082–3.

[15] Worth ER, Burton RJ, Landreneau RJ, Eggers GWN, et al. Left atrial air embolism during intraoperative needle biopsy of a deep pulmonary lesion. Anesthesiology 1990;73:342–5.

[16] Wong RS, Ketai L, Temes RT, Follis FM, et al. Air embolus complicating transthoracic percutaneous needle biopsy. Ann Thorac Surg 1995;59:1010–1.

[17] Khatri S. Cerebral artery gas embolism (CAGE) following fine needle aspiration biopsy of the lung. Aust NZ J Med 1997;27. pp. 27–27.

[18] Regge D, Gallo T, Galli J, et al. Systemic arterial air embolism and tension pneumothorax: two complications of transthoracic percutaneous thin-needle biopsy in the same patient. Eur Radiol 1997;7:173–5.

[19] Kodama F, Ogawa T, Hashimoto M, et al. Fatal air embolism as a complication of CT-guided needle biopsy of the lung. JCAT 1999;23:949–51.

[20] Shetty PG, Fatterpekar GM, Manohar S, et al. Fat cerebral air embolism as a complication of transbronchoscopic lung biopsy: a case report. Aust Radiol 2001;45:215–7.

[21] Arnold BW, Zwiebel WJ. Percutaneous transthoracic needle biopsy complicated by air embolism. AJR Am J Roentgenol 2002;178:1400–2.

[22] Mokhlesi B, Ansaarie I, Bazen B, et al. Coronary artery air embolism complicating a CT-guided transthoracic needle biopsy of the lung. Chest 2002;121:993–6.

[23] Laurent F, Montaudon M, Latrabe V, et al. Percutaneous biopsy in lung cancer. Eur J Radiol 2003;45:60–8.

[24] Ohi S, Ito Y, Keiya H, et al. Air embolism following computed tomography-guided lung needle marking; report of a case. Kyobu-Geka 2004;57:421–3.

[25] Kamiyoshihara M, Sakata K, Ishikawa S, et al. Cerebral arterial air embolism following CT-guided lung needle marking; report of a case. J Cardiovasc Surg 2001;42:699–700.

[26] Sakiyama S, Kondo K, Matsuoka H, et al. Fatal air embolism during computed tomography-guided pulmonary marking with a hook-type maker. J Thorac Cardiovasc Surg 2003;126:1207–9.

[27] Muller NL, Bergin CJ, Miller RR, et al. Seeding of malignant cells into the needle track after lung and pleural biopsy. J Can Assoc Radiol 1986;37:192–4.

[28] Redwood N, Beggs D, Morgan WE. Dissemination of tumor cells from fine needle biopsy. Thorax 1989;44:826–7.

[29] Berger RL, Dargan EL, Huang BL, et al. Dissemination of cancer cells by needle biopsy of the lung. J Thor Cardiovasc Surg 1972;63:430–2.

[30] Freise G, Larios R, Takeno Y, et al. Cell dissemination and implantation of neoplasms through biopsy and excision of malignant tumors. Dis Chest 1967;52:485–9.

[31] Christensen ES. Iatrogenic dissemination of tumor cells. Dissemination of tumour cells along the needle track after percutaneous, transthoracic lung biopsy. Danish Med Bull 1978;25:82–7.

[32] Ferrucci JT, Wittenberg J, Margolies MN, et al. Malignant seeding of the tract after thin-needle aspiration biopsy. Radiology 1979;130:345–6.

[33] Yoshikawa T, Yoshida J, Nishimura M, et al. Lung cancer implantation in the chest wall following percutaneous fine needle aspiration biopsy. Jpn J Clin Oncol 2000;30:450–2.

[34] Kara M, Alver G, Sak SD, Kavukcu S. Implantation metastasis caused by fine needle aspiration biopsy following curative resection of stage IB non-small cell lung cancer. Eur J Cardiothor Surg 2001;20:868–70.

[35] Ayar D, Golla B, Lee JY, Nath H. Needle-track metastasis after transthoracic needle biopsy. J Thorac Imag 1998;13:2–6.